Int. J. Electrochem. Sci., 2 (**2007**) 734 - 746

International Journal of ELECTROCHEMICAL SCIENCE
www.electrochemsci.org

Deposition and Dissolution of Cr-P Alloy: A Cyclic Voltammetric Approach

C. N. Tharamani[1,2,*], *V. S. Murulidharan*[3], *and S. M. Mayanna*[2,**]

[1] Department of Chemistry, University of Saskatchewan, Saskatoon, SK S7N5C9, Canada
[2] Department of Post-Graduate studies and Research in Chemistry, Central College, Bangalore University, Bangalore -560 001, India
[3] Central Electrochemical Research Institute, Karaikudi, 630 006, India
[*]E-mail: thara9@gmail.com
[**]E-mail: Smm_chem@yahoo.com

Received: 16 June 2007 / *Accepted:* 14 July 2007 / *Published:* 1 October 2007

Cyclic voltammetric experiments were carried out on platinum microelectrode in acidic solution (pH 3.0) containing chromium sulphate, potassium thiocyanate and sodium hypophosphite. Spectral U.V. absorption studies indicate the complexation of Cr^{3+} with potassium thiocyanate. The deposition of Cr involves a stepwise reduction mechanism. The results under transient polarization conditions infer the reduction of Cr^{2+} ions with second electron transfer as a slow step. The observed cyclic voltammetric data show that the alloy deposition is possibly from Cr-complex. Stripping voltammograms show the existence of chromium rich alloy phases. X-ray diffraction data further confirms the phases to be Cr_3P and $Cr_{12}P_7$.

Keywords: Electrodeposition, Cr-P alloy film, Cyclic voltammetry, U.V. absorption, XRD studies.

1. INTRODUCTION

Chromium is a versatile metal because it sustain tarnish, corrosion, wear and scratch resistance even under severe service conditions and provides an oxide film with decorative appeal [1]. The process of development suffers several drawbacks from environmental and economical points of view [2]. Despite many developments have been reported in this field, there is no comprehensive approach made to the problem [3, 4]. Chromium deposition from plating bath solution containing trivalent chromium is of current interest [5]. Phosphorous being a metalloid, addition of which to chromium imparts better corrosion resistance [6].

Cyclic voltammetry is a versatile experimental technique used in the understanding of reaction pathways [7]. However, its use for alloy deposition process is found to be limited [8-10]. The objective

of the present work is to analyse the plating bath solution used for deposition of Cr-P alloys by cyclic voltammetric technique. In the earlier paper [11, 12] we reported the microstructure, surface properties and corrosion resistance of Cr-P alloy coating. Platinum microelectrode is used to decrease the effects of uncompensated IR drops, charging currents and enhance the mass transport process. These make it possible to work in the high bath concentration range associated with the plating process and obtain currents controlled by diffusion in the presence of convective mass transport [13]. Attempts are made to understand the electrochemical behaviour of plating bath solution under acidic condition containing chromium sulphate, sodium hypophosphite and KCNS (complexing agent). U.V. absorption spectral and XRD techniques are used to correlate the observed results.

2. EXPERIMENTAL PART

2.1. Apparatus

Experiments were carried out in an all glass single compartment cell of 50ml capacity at 298K. A micro platinum electrode was used as a working electrode along with a large platinum foil and saturated calomel electrode as auxiliary and reference electrodes respectively. A luggin capillary was used to minimize the IR drop. The platinum electrodes were precleaned by a standard procedure [14]. Cyclic voltammograms were obtained at various scan rates (10 - 100 mV/sec) by monitoring the desired potential using a potentiostat (EG & G PAR 362) and only reproducible CV responses were recorded. Ultraviolet absorption studies were made using a spectrometer (Hitachi 150-20, Japan). An X-ray diffractometer [(Philips, PW 1140/90) CuK_{α} radiation] was used to characterize the deposited alloy phases.

2.2. Reagents

All solutions were prepared using double distilled water and AR grade chemicals. Potassium thiocyanate (KCNS) of known concentration ($0.05M < x < 0.15M$) was used along with chromium sulphate [$Cr_2(SO_4)_36H_2O$ (0.1M)], Sodium hypophosphite [NaH_2PO_2 ($0.1M < x < 0.02M$)], sodium chloride [NaCl (0.17M)], boric acid [H_3BO_3 (0.05M)]. The pH of the medium was maintained at 3.0 by adding dilute H_2SO_4.

3. RESULTS

3.1. Preliminary results

The cyclic voltammograms were fdg dfhg dgfg obtained on platinum in a wide range of potential (-1500 to + 1500 mV) at different scan rates (10-100 mV s^{-1}). For a comparison purpose, suitable scan rate is selected to have a better feature of cyclic voltammogram.

The voltammogram from a solution containing Cr^{3+} ions but no phosphorus is shown in Figure 1. During forward and reverse scans, several peaks appear at different potentials which are

characteristics of typical electrode reactions. Aqueous solution chemistry of Cr is very complex having species of different oxidation states [15] and also oxides and hydroxides derived because of drastic change in pH at the vicinity of electrode. These species are active at the electrode surface at different potentials and the respective current is a measure of the reaction rate. During forward scan, the cathodic current increased sharply at –1200 mV and the trace was typical for an electrode reaction most possibly the evolution of H_2 gas (reaction 1).

$$2H^+ + 2e \longrightarrow H_2 \quad (1)$$

This is followed by deposition of Cr from the reactions (2) and (3) at –900 mV and –650 mV respectively.

$$Cr^{2+} + 2e \longrightarrow Cr \quad (2)$$

$$Cr^{3+} + 3e \longrightarrow Cr \quad (3)$$

The rest potential was found at –250 mV. During reverse scan, an anodic stripping peak is obtained at 700 mV (reaction 4) followed by oxygen evolution (reaction 5) at 1000 mV.

$$Cr \longrightarrow Cr^{3+} + 3e \quad (4)$$

$$2H_2O \longrightarrow O_2 + 4H^+ + 4e \quad (5)$$

To know the anodic behaviour of Cr, cyclic voltammograms (Figure 2) were obtained from a solution containing supporting electrolyte using coated Cr and also platinum as electrodes. The rest potential of Cr in this solution is –250 mV and anodic peak starts from this potential as in Figure 1. Evolution of H_2 takes place slightly at lower potential on Cr than on platinum in H_2SO_4.

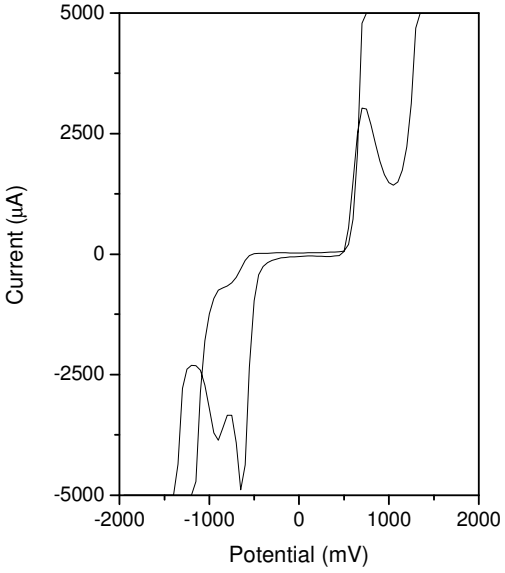

Figure 1. Cyclic voltammograms obtained from the solution containing Cr^{3+} in the absence of P at a scan rate of 25 mV s^{-1}.

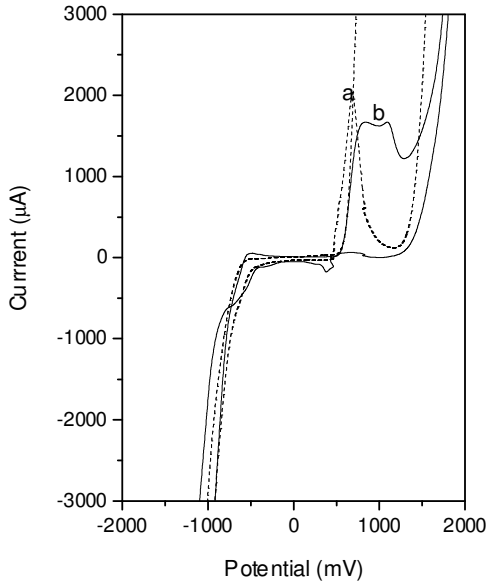

Figure 2. Cyclic voltammograms on Cr and Pt in the plating solution containing supporting electrolyte at a scan rate of 25 mV s^{-1} (a) NaCl + H_3BO_3 (dashed lines) (b) H_2SO_4 (1N, full lines).

3.2. Influence of supporting electrolyte and potassium thiocyanate

A typical cyclic voltammogram obtained in conducting salt and buffering agent at a scan rate 25 mV s^{-1} is shown in Figure 3a. It is possible to explain the feature of the observed cyclic voltammogram with the help of our earlier findings [16]. During the forward scan a small an anodic peak (a_1) was observed at -350 mV, followed by two significant cathodic peaks at +950 mV [c_1(I)] and +100 mV [c_1(II)]. Notable increase in the anodic current at 1200 mV is due to the oxidation of the chloride ions.

$$2Cl^- \longrightarrow Cl_2 + 2e \quad (6)$$

Further steep rise in current with an increase in potential is due to the evolution of O_2

$$2H_2O \longrightarrow O_2 + 4H^+ + 4e \quad (7)$$

During the reverse scan, reduction of Cl_2 [reverse reaction of (I)] takes place [c_1(I)] probably through consecutive steps [17].

$$Cl_2 + e \longrightarrow Cl_{ads} + Cl^- \quad (8)$$

$$Cl_{ads} + e \longrightarrow Cl^- \quad (9)$$

The evolved or absorbed O_2 species by the reaction (7) is reduced in the cathodic scan producing peak c_1(II) [18].

It is known that H_2 evolution reaction occurs reversibly on platinum surface at low pH and a negative potential from water

$$2H_2O + 2e \longrightarrow H_2 \quad (10)$$

In the present system, the cathodic peak current increases significantly with the increase in H_3BO_3 concentration. Thus it is likely that the reduction of H_3BO_3 to diborane occurs at this potential [19].

$$2H_3BO_3 + 2H^+ + 12e \longrightarrow B_2H_6 + 6\,H_2O \quad (11)$$

The diborane solution becomes hydrogen saturated through the hydrolysis reaction [20].

$$B_2H_6 + H_2O \longrightarrow H_3BO_3 + H_2 \quad (12)$$

Anodic oxidation of diborane ion is known to ionise the evolved H_2 [21]. With these consecutive steps, H_3BO_3 retards the rate of H_2 evolution during plating.

The role of KCNS in the bath solution can understood from the electrochemical characteristics obtained in 0.1M solution (Figure 3b). During forward and reverse scans at a scan rate of 25 mV s^{-1}, anodic peak (a_2) and cathodic peak (c_2) were recorded at +750 mV and –550 mV respectively. The appearance of these peaks are attributed to the oxidation of adsorbed H_2 atoms produced during cathodic cycle. H_2 evolution takes place at more negative potential.

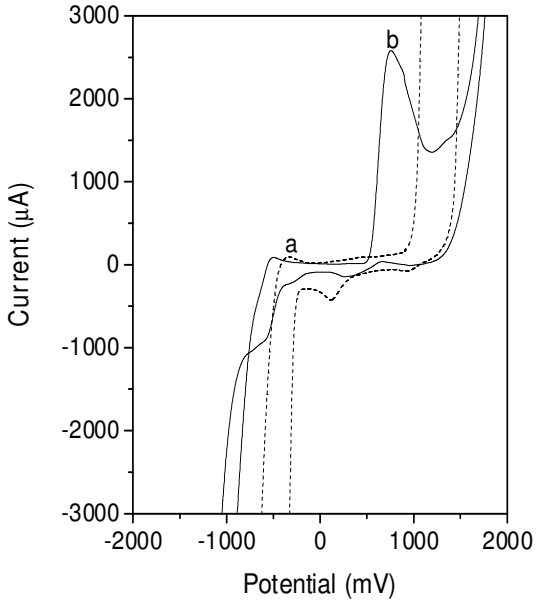

Figure 3. Cyclic voltammograms obtained at a scan rate of 25 mV s^{-1} in solution containing (a) 0.17M NaCl + 0.05M H_3BO_3 (dashed lines) 0.1M KCNS (full lines).

3.3. Influence of Cr^{3+} ions with KCNS and sodium hypophosphite

Figure 4. shows the electrochemical characteristics obtained in 0.1M $Cr_2(SO_4)_3$ and 0.1M KCNS solutions at various sweep rates is shown in Figure 4a, b, c. During the forward scan, anodic peak appeared at 600 mV, which became nobler with increase in scan rate. While reverse in the scan,

cathodic peak appeared at -600 mV followed by hydrogen evolution. The cathodic peak potential due to the reduction of trivalent chromium ions became appreciable with scan rate. Electrochemical characteristics obtained at various conc. of KCNS (Figure 5) revealed that anodic peak potential is constant with concentration. While reversing the scan, zero current crossing potential (ZCCP) became noble, while cathodic peak potentials were constant. Anodic and cathodic peak currents increased with KCNS concentration suggesting that dissolution of chromium and deposition of chromium were affected by KCNS concentration.

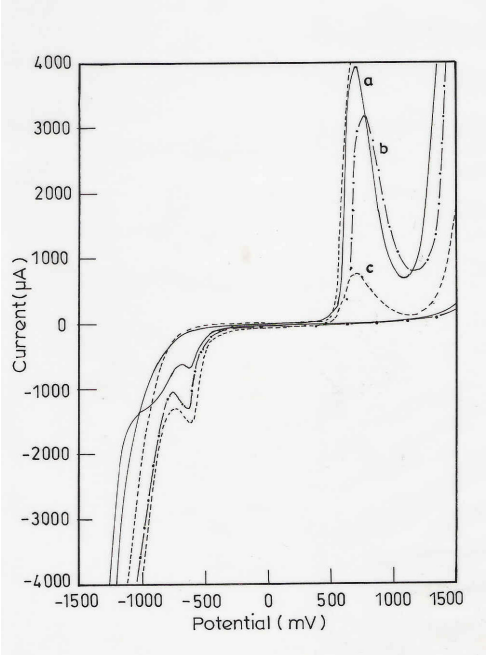

Figure 4. Cyclic voltammograms obtained in 0.1M $Cr_2(SO_4)_3$ with 0.1M KCNS at various sweep rates (a) 10, (b) 25 and (c) 50 mV s^{-1}.

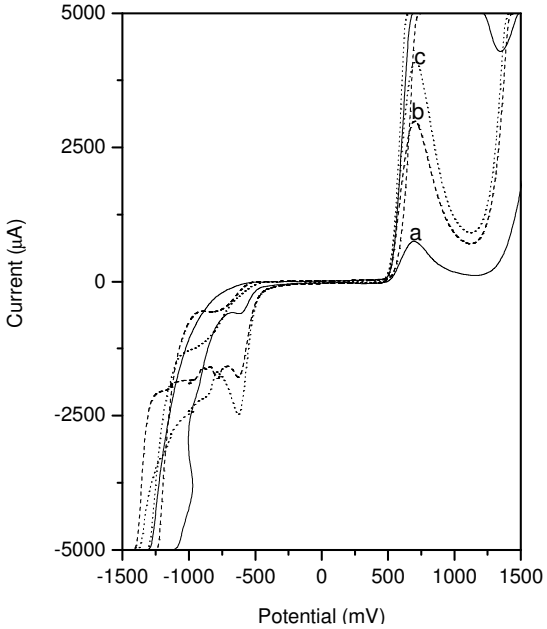

Figure 5. Cyclic voltammograms obtained in solution [with 0.17M NaCl + 0.05M H_3BO_3 at 25mV s^{-1}] 0.1M $Cr_2(SO_4)_3$ containing various concentration of KCNS (a) 0.05M (b) 0.1M and (c) 0.15M.

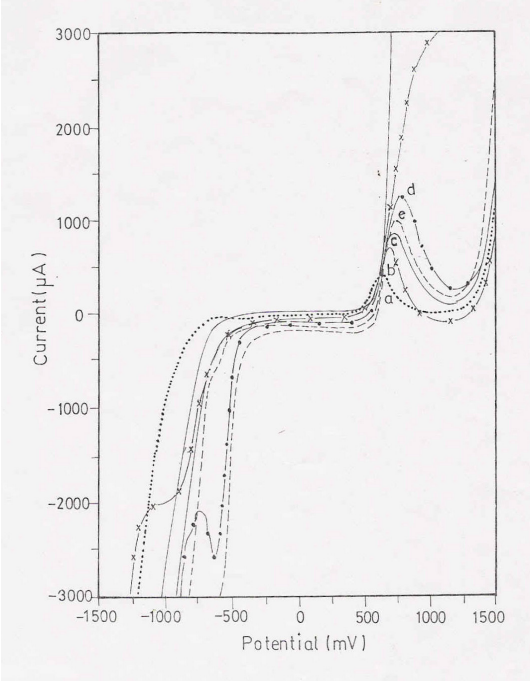

Figure 6. Cyclic voltammograms obtained in solution containing 0.1M $Cr_2(SO_4)_3$ + 0.1MKCNS + 0.1M NaH_2PO_2 + 0.17M NaCl + 0.05M H_3BO_3 at various sweep rates (a) 5, (b) 10, (c) 25, (d) 50 and (e) 100 mV s^{-1}

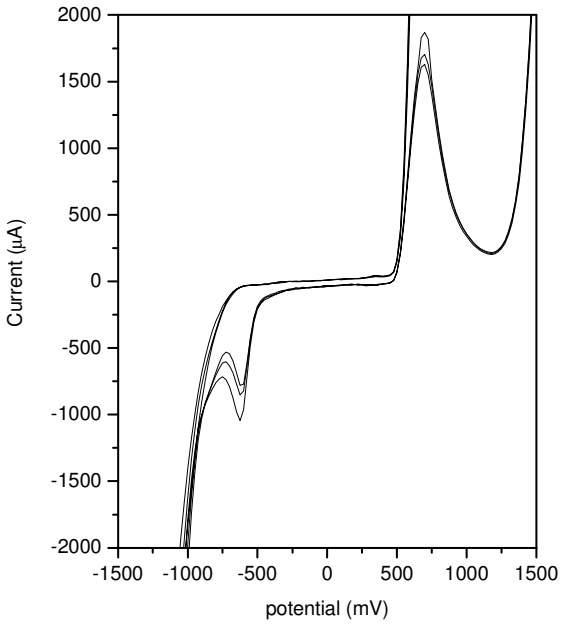

Figure 7. Effect of cycling on cyclic voltammograms obtained in solution containing 0.1M $Cr_2(SO_4)_3$ + 0.1M KCNS + 0.1M NaH_2PO_2 + 0.17M NaCl + 0.05M H_3BO_3 at a scan rate of 25 mV s^{-1}.

Figure 6 shows the electrochemical characteristics obtained in 0.1M NaH_2PO_2 solutions containing Cr^{3+} ions and KCNS. During the forward scan an anodic peak was observed at 675 mV followed by oxygen evolution at a scan rate of 25 mV s^{-1}. Increase of scan rate shifted the peak

potentials in nobler direction. While reversing the scan a cathodic peak was observed at -625 mV at 25 mV s^{-1} and peak potentials became active with scan rate. The observed anodic peak may be due to dissolution of chromium alloy along with NaH_2PO_2 oxidation. The cathodic peak obtained at -625 mV is due to the reduction of dissolved chromium complexes followed by hydrogen. In the second and third cycles, anodic peak appeared at 700 mV due to the oxidation of $H_2PO_2^-$ ion when the scan was reversed, cathodic peak appeared at –650 mV due to the reduction of oxidized product of $H_2PO_2^-$ ion followed by H_2 evolution (Figure 7).

Increase of NaH_2PO_2 concentration did not affect the anodic peak potential but decreased the peak current suggesting that chromium alloy dissolution is not favoured. While reversing the scan, the observed ZCCP at 540 mV became nobler, with increase in cathodic peak, shifting the peak potentials to negative direction (Figure 8) suggest deposition of chromium alloy being favoured.

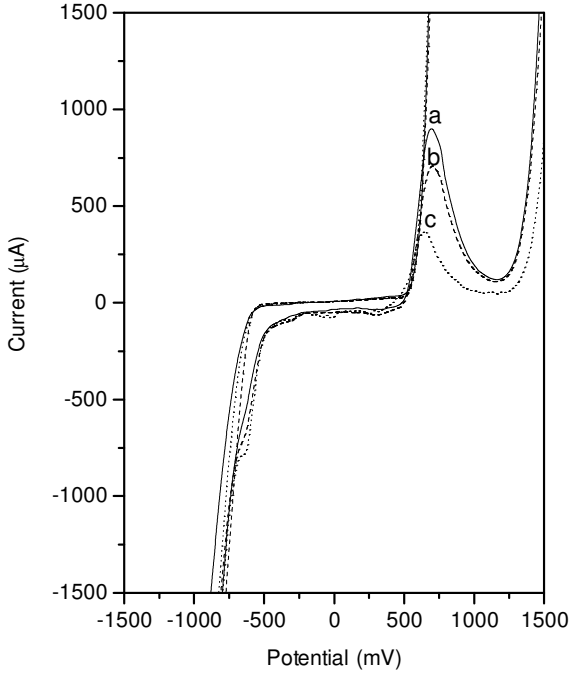

Figure 8. Cyclic voltammograms obtained in solution [with 0.17M NaCl + 0.05M H_3BO_3 at 25mV s^{-1}] 0.1M $Cr_2(SO_4)_3$ containing various conc. of NaH_2PO_2 (a) 0.1M, (b) 0.15M and (c) 0.2M.

3.4. UV absorption spectral and XRD studies

Chromium +3 forms number of complexes in which it is surrounded by neutral ligands likes water molecules and anions octahedrally [22]. Polarographic analysis revealed that Cr^{3+} form complex with KCNS [23]. UV absorption spectra (Figure 9) of an aqueous solutions of Cr^{3+} ions containing KCNS exhibits 3 bands around 17543, 24450 and 37660 cm^{-1} which are characteristics of $^4A_{2g} \rightarrow {}^4T_{2g}$, $^4A_{2g} \rightarrow {}^4T_{1g}$ (F) and $^4A_{2g} \rightarrow {}^4T_{1g}$ (P) transitions corresponding to a metal ligand complex of octahedral geometry. XRD data were obtained for alloys from various Cr:P (molar ratio) solutions. The phases and compounds identified from these data are indicated in Table1.

Table 1. XRD data obtained* on Cr-P codeposits

Solution Cr:P molar ratio	*2θ*	*d/nm*	*Phases*
	36.55	2.46	CrP (111)
	42.09	2.15	Cr_3P (112)
1:1	48.20	1.88	CrP (103)
	49.71	1.83	P (121)
	74.89	1.27	Cr_3P (413)
	28.83	3.10	$Cr_{12}P_7$ (210)
	34.63	2.58	$Cr_{12}P_7$ (300)
1:1.5	47.18	1.92	$Cr_{12}P_7$ (400)
	50.52	1.80	$Cr_{12}P_7$ (311)
	72.86	1.30	Cr_3P (323)
	34.59	2.59	$Cr_{12}P_7$ (300)
	44.17	2.04	$Cr_{12}P_7$ (301)
1:2	47.43	2.18	$Cr_{12}P_7$ (211)
	50.47	1.81	P (121)
	74.16	1.27	p (222)

* CuK_α radiation

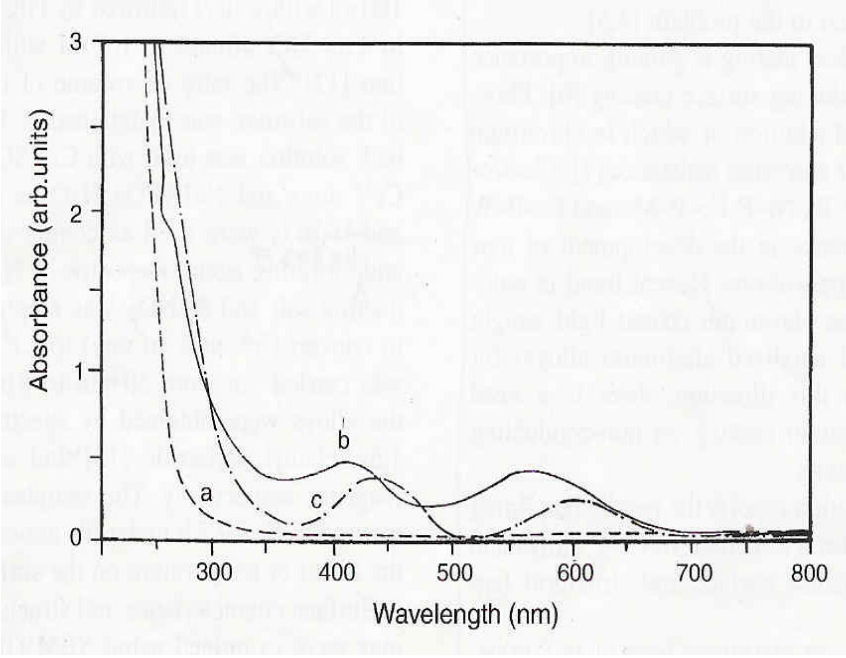

Figure 9. UV absorption spectra of solutions: (a) KCNS (b) Cr^{3+}+ KCNS (c) Cr^{3+}+ KCNS+ NaH_2PO_2.

4. DISCUSSION

4.1. Deposition of Chromium

Most Cr^{3+} complexes undergo stepwise charge transfer at the electrode in which the second step of Cr^{2+} reduction is slow [24]. Various halides are effective bridging ligands which assist the electron transfer between metal ions and the electrode [25].

In the present study the deposition chromium under transient polarization conditions (10 - 100 mV s^{-1}) may involve the Cr(II) formation and may occur as

$$[Cr(CNS^-)]^{3+} + e \longrightarrow [Cr(CNS^-)]^{2+} \quad (13)$$

if the first electron transfer is slow

$$i_c = K[Cr(III)] \exp^{-\alpha c F \Delta\phi\bar{c}RT} \quad I$$

where α_c is cathodic transfer co-efficient; $\Delta\phi_c$ is the interfacial potential difference. If the discharge is irreversible.
(as there is no anodic peak)

$$E_{p,c} = E^o + RT/nF [\log k^o/\sqrt{d} - 0.5 \ln \alpha_c F\nu RT - 0.78] \quad II$$

where $E_{p,c}$ is the cathodic peak potential; E^o is the formal potential; α_c is the cathodic transfer co-efficient; ν is the diffusion co-efficient of Cr(III) ions. A plot of $E_{p,c}$ vs logν would give cathodic Tafel slope. An observed $E_{p,c}$ vs logν linear plot with a slope of 130 mV $decade^{-1}$ (Figure 10) confirms the first electron transfer as rds.

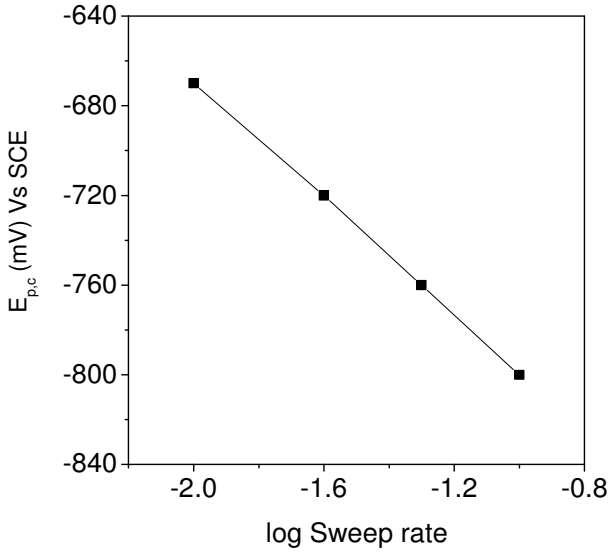

Fig. 10 Variation of cathodic peak potentials with log sweep rate in 0.1M $Cr_2(SO_4)_3$ + 0.1M KCNS solutions.

4.2. Deposition of Cr-P alloy

In slightly acidic solution, chromium thiocyanate complex gets reduced to chromium. The deposition of Cr-P alloy is a complex process similar to Ni-P alloy deposition [26] involving several intermediate species and hydrogen.

In the present study $H_2PO_2^-$ ion reduces to P and it can be oxidized to $H_2PO_3^-$ ion by coupled chemical reaction [27].

$$H_2PO_2^- + 2H^+ + 2e \rightleftharpoons P + H_2O \quad (14)$$

$$H_2PO_2^- + H_2O \rightleftharpoons H_2PO_3^- + H_2\uparrow \quad (15)$$

$$H_2PO_2^- + 5H^+ + 4e \rightleftharpoons PH_3 + 2H_2O \quad (16)$$

In the case of alloy deposition,

$$2H_2O + 2e \rightarrow H_2 + 2OH^- \quad (17)$$

$$[Cr(CNS^-)]^{2+} + 2OH^- \rightarrow [Cr(OH)_2] + CNS^-$$

$$[Cr(OH)_2] + [H_2PO_3]^{2-} \rightarrow [Cr(PO_3)] + 2H_2O + H_2\uparrow + 2H^+ \quad (18)$$

$$x\ PH_3 + y\ [Cr(OH)_2] + z\ H_2O \rightarrow l\ \text{Cr-P alloy} + m\ H^+ + \text{phosphorous oxy acids} \quad (19)$$

the values of x, y, z, l, m would vary with the type of Cr-P alloy formed.

4.3. Hydrogen evolution reaction

During electrodeposition hydrogen evolution involves charge transfer of water molecules and desorption of adsorbed H_2 either by electrochemical or chemical reaction pathways. While most of molecular H_2 is removed from the electrode surface, a fraction of it becomes adsorbed and may get incorporated in the lattice of the electrode surface. Figure 10 shows the linear sweep voltammetric curves obtained in different Cr:P (molar ratio) solutions. Hydrogen evolution reaction rate gets enhanced by the incorporation of P into Cr and with increase in the concentration of $H_2PO_2^-$ ions.

4.4. Dissolution of Cr-P alloy

Table 2 summarizes the parameters derived from cyclic voltammograms for chromium dissolution. The anodic peak potential being nobler with P content than with that of chromium could be attributed to one of the two reasons. There may be a significant free energy change of mixing or some kinetic factor may have caused the shift in the peak away from its reversible potential in the positive direction. The dissolution of chromium may take place from the intermediate phases formed during deposition.

Table 2. Parameters obtained from cyclic voltammograms for Cr-P dissolution

Solution Cr:P molar ratio	*Anodic peak potential (mV)*	*Anodic peak intersection potential (mV)*
1:0	675	500
1:1	750	475
1:1.5	700	450
1:2	650	425

Solution composition/M : 0.1M $Cr_2(SO_4)_3$; 0.1M KCNS; 0.1M NaH_2PO_2; 0.17M NaCl; 0.05M H_3BO_3, pH 3.0 at 25 mV s^{-1}.

5. CONCLUSIONS

Electrodeposition of Cr-P alloys on platinum was studied from $Cr_2(SO_4)_3$, NaH_2PO_2, H_3BO_3 and NaCl solutions. U.V. absorption spectra revealed the formation of trivalent octahedral chromium thiocyante complex. The reduction of the chromium complex to chromium involves the formation of divalent chromium complex whose formation is slow. The Cr-P alloy deposits were associated with various phases of phosphorus and chromium. The crystalline deposit exhibited single dissolution peak suggesting that dissolution taking place from various phases simultaneously. The formation of these phases involves divalent chromium hydroxide, and PH_3. Hydrogen evolution was found to occur faster on Cr-P alloy surface than on chromium.

ACKNOWLEDGMENTS
One of the authors (SMM) expresses his gratitude to the AICTE, New Delhi for the financial assistance.

References

1. D.R. Gabe, Metal Finishing Guide Book, Elsevier Inc., New York, 1998.
2. J.K. Dennis, T.E. Such, Nickel and Chromium Plating, Butterworths, London**,** 186, 1972.
3. A. Watson, M.H. Anderson, M.R. El-sharif, C.U. Chisholm, *Trans. Inst. Metal Finish***.** 68 (1990) 26.
4. M. Paunovic, (Eds: Schlesingen M) Fundamentals of Electrochemical Deposition-The Electrochemical Society Series, Wiley-Interscience Publication, John Wiley & Sons, Inc., New York, 1998.
5. J. McDougall, M. El-Sharif, S. Ma, *J. Appl. Electrochem.* 28 (1998) 929.
6. T. Watanabe, Y. Sakurai, Y. Hamakaw, T. Masumoto, K. Shirae, K. Suzuki (Eds.), Current Topics in Amorphous Materials-Physics and Technology, Elsevier Science Publishers, New York, 137, 1993.
7. P.T. Kissinger, W.R. Heineman, *J. Chem. Edu*. 60 (1983) 702.

8. K. Wikiel, J. Osteryoung, *J. Appl. Electrochem*. 22 (1992) 506.
9. C.L. Aravinda, V.S. Murulidharan, S.M. Mayanna *J. Appl. Electrochem*. 30 (2000) 601.
10. C.L. Aravinda, V.S. Murulidharan, S.M. Mayanna, *J. Appl. Electrochem*. 30 (2001) 1227.
11. C. N. Tharamani, Noor Shahina Begum, S. M. Mayanna, *Materials Chemistry and Physics* 83 (2-3) (2004) 278.
12. C. N. Tharamani, F. Shafia Hoor, Noor Shahina Begum, S. M. Mayanna, *Journal of Solid State Electrochemistry* 9(7) (2005) 476.
13. N. Howarth, D. Pletcher, *J. Appl. Electrochem*. 22 (1992) 506.
14. R. Greef, R. Peat, L.M. Peter, D. Pletcher (Eds: J. Robinson), Instrumental Methods in Electrochemistry, Ellis Horwood, Chichester, p.359, 1985.
15. David R. Lide, Hand Book of Chemistry and Physics, (Edn: 76th), CRC press 1995-96.
16. T. Mimani, S.M. Mayanna, N. Munichandraiah, *J. Appl. Electrochem*. 23 (1993) 339.
17. A. N. Frumkin and G. A. Tedoradze, *Z. Elektrochem*.62 (1958) 251.
18. J.P. Hoare, The Electrochemistry of Oxygen, Ch. II, John Wiley & Sons, p. 29 (1968).
19. M.I. Bellarance, B. Miller, in Encyclopedia of the Electrochemistry of the Elements, Ch. I (Edited by Allen J. Bard), Marcel Dekkar Inc. New York, p.2, 1975.
20. F.A. Cotton, G. Wilkinson, Advanced Inorganic Chemistry, 3rd Edn., Ch. 8, John Wiley & Sons, part 2, p. 239, 1972.
21. J.P. Elder, *Electrochim. Acta* 7 (1962) 417.
22. W.W. Porterfeld (Ed.) Inorganic Chemistry – A Unified Approach, Wesley Publishing Co. New York, 1984.
23. E. Fischerova, O. Fischer, *Collection Czech. Chem. Commun.* 26 (1961) 2570.
24. Allen J. Bard (Ed.), Encyclopedia of Electrochemistry of the Elements, Vol.9, Part B, Marcel Dekkar Inc., New York, 1986.
25. J.B. Wills, *J. Proc. R. Soc. NSW* 78 (1994) 239.
26. T. Mimani, S.M. Mayanna *Proc. Ind. Acad. Sci. (Chem. Sci.)* 109 (1997) 203.
27. Pourbaix M (Ed.), Atlas of Electrochemical Equilibria in Aqueous Solutions, Pergamon Press, New York, 1966.